Journal of Solid State Chemistry 183 (2010) 1165–1173

Contents lists available at ScienceDirect

Journal of Solid State Chemistry

journal homepage: www.elsevier.com/locate/jssc

Structural variations of Sn^{II} pyridylphosphonates influenced by an uncommon Sn–N interaction

Houston Perry [a], Jerzy Zoń [b], Justin Law [a,1], Abraham Clearfield [a,*]

[a] Dept. of Chemistry, Texas A&M University, College Station, TX, USA
[b] Faculty of Chemistry, Wroclaw University of Technology, Wroclaw, Poland

ARTICLE INFO

Article history:
Received 14 October 2009
Received in revised form
4 March 2010
Accepted 8 March 2010
Available online 12 March 2010

Keywords:
Tin phosphonates
Pyridylphosphonic acids
Hybrid materials

ABSTRACT

Four new Sn^{II} phosphonates have been synthesized by hydrothermal methods, and their structures determined by single-crystal X-ray diffraction. Tin(II) 3-pyridylphosphonate, $SnO_3PC_5H_4N$ (**I**), crystallizes in $P2_1/c$ with $a=4.9595(8)$ Å, $b=10.7673(18)$ Å, $c=13.996(2)$ Å, and $\beta=93.616(2)^\circ$. Tri-tin(II) (μ-3)-oxo-(bis)-4-pyridylphosphonate, $Sn_3O(O_3PC_5H_4N)_2$ (**II**), crystallizes in P-1 with $a=7.2406(14)$ Å, $b=9.9524(19)$ Å, $c=12.604(3)$ Å, $\alpha=104.510(11)^\circ$, $\beta=90.326(11)^\circ$, and $\gamma=110.897(11)^\circ$. Tin(II) 6-methyl-2-pyridylphosphonate quadrahydrate, $Sn(O_3PC_5H_3NCH_3)\cdot 0.25H_2O$ (**III**), crystallizes in $Pna2_1$, $a=18.955(3)$ Å, $b=9.7543(14)$ Å, and $c=17.833(3)$ Å. Tin(II) 4-cyanophenylphosphonate, $Sn(O_3PC_6H_4CN)$ (**IV**), crystallizes in P-1, $a=5.0019(3)$ Å, $b=8.4396(5)$ Å, $c=10.3099(6)$ Å, $\alpha=90.352(3)^\circ$, $\beta=94.894(3)^\circ$, and $\gamma=92.236(4)^\circ$. **I**, **II**, and **IV** have ladder-type structures, and **III** is a layered compound. The structural variations show the effects of the Sn–N interaction on the final structures.

1. Introduction

The term 'hybrid material' is used to refer to a member of the broad class of materials that possess both inorganic and organic constituents. Included in this classification are crystalline 'metal organic frameworks' (MOFs) [1–10], as well as semi-amorphous, pillared, layered compounds such as Zr 4,4′-biphenyldiylbisphosphonate and its Sn^{IV} analogue [11–13]. In both of these types of compounds, the inorganic units are covalently bound to the organic moieties of the structure, which can also contain other functional groups. Hybrid materials show great potential in a variety of applications including gas storage [14,15], gas separations [16], catalysis [13,17,18], and ion exchange [19]. The viability of most of these applications depends on the nanoscale structural characteristics of the material. Compounds with potential in hydrogen storage or gas separation rely on the surface area or porosity as the main source of functionality. On the other hand, supported catalysts and ion exchangers require a chemically active moiety such as –COOH or $–NH_2$ to impart additional chemical properties.

Metal complexes and extended networks utilizing pyridylphosphonic acids are promising candidates for functional materials, and they have been the topic of several recent papers. Lin et al. synthesized and characterized several compounds of Zn, Co, Cu, and Cd with 3- and 4-pyridylphosphonic acids [20]. By using the hydrobromide of 3-pyridylphosphonic acid, they obtained a ladder structure in which the Zn atom is four-coordinate and the pyridyl nitrogen atom is protonated. The N atoms of the pyridyl ring in Co(4-pyridylphosphonate)$(H_2O)_3$ coordinate the Co atoms, which are also coordinated by three water molecules. The N–Co coordination links the chains of CoO_5N and PO_3C polyhedra, forming a 2-D grid network. Cu_2(4-pyridylphosphonate)$_2\cdot 2H_2O$ forms a 3-D network that possesses open channels occupied by water molecules. An interesting Cd compound was obtained by using diethyl 4-pyridylphosphonate. By keeping the temperature low (70 °C), they avoided the complete hydrolysis of the ester and obtained the compound Cd(*O*-ethyl-4-pyridylphosphonate)$_2$, in which the ethyl groups occupy the voids within the 3-D network.

Anne Richards and her coworkers [21] have prepared a variety of interesting compounds with Zn, Cd, Hg, and Ag, utilizing 2-pyridylphosphonic acid under mild conditions. The compounds illustrate some of the many possible binding modes for phosphonates. Cd(μ-Cl)$_2$(2-pyridylphosphonate) has chloride ions which bridge between Cd atoms. By reacting silver triflate with 2-pyridylphosphonic acid in ethanol they obtained a compound in which silver chains are coordinated by both phosphonate and triflate oxygen atoms.

Li-Min Zheng et al. have also used 2-pyridylphosphonic acid to prepare a trio of copper compounds [22]. In each of the structures, the pyridyl nitrogen atoms are bound to the Cu^{II} ions. $Cu(C_5H_4NPO_3H)_2$ forms chains, while $Cu_3(OH)_2(C_5H_4NPO_3)_2\cdot 2H_2O$ and $Cu(C_5H_4NPO_3)$ form layered structures. They have also reported

* Corresponding author at: Dept. of Chemistry, Texas A&M University, Corner of Spence and Ross, College Station, TX 77843-3255, USA. Fax: +1 979 845 2370.
E-mail address: Clearfield@mail.chem.tamu.edu (A. Clearfield).
[1] Undergraduate Researcher.

0022-4596/$ - see front matter © 2010 Elsevier Inc. All rights reserved.
doi:10.1016/j.jssc.2010.03.016

[23] the syntheses of a Mn derivative of 2-pyridylphosphonic acid and a Zn derivative of 6-methyl-2-pyridylphosphonic acid by hydrothermal methods. $Mn(C_5H_4NPO_3)_2(H_2O)$ and Zn(6-Me-2-$C_5H_4NPO_3$) are both layered compounds in which the pyridyl groups occupy space between the layers.

Recently we explored the compounds formed by Zn, Mn, and Cu with 4-pyridylphosphonic acid [24]. In the Zn compound, the tetrahedral Zn atoms are bound to two Cl atoms and two phosphonate O atoms. Two Zn atoms are bridged by O–P–O linkages to form eight-membered rings, but the two Cl atoms prevent edge-sharing of the rings and formation of ladders. The pyridyl nitrogen atoms are protonated and engage in hydrogen bonding with phosphonate oxygen atoms. The Mn compound forms layers that are linked by pendant pyridyl groups, while the Cu compound forms a 3-D network that contains interpenetrating channels along all three crystallographic axes. The channels are filled with solvent water molecules that contribute to the stability of the compound.

Although pyridylphosphonic acids have yielded a panoply of coordination polymers with divalent metals, there have been no studies on the compounds they form with Sn^{II}. These compounds may be of use in ion exchange and catalysis, as they contain potentially active lone pairs. A variety of structural motifs have been observed for Sn^{II} phosphonates, including chains [25], rings, ladders (edge-sharing rings), and sheets [26]. Cheetham and coworkers [27] have developed a system of nomenclature for the inorganic units formed in these structure types, which describes them in terms of the number of Sn and P atoms in the Sn–O–P–O rings. The most prevalent rings are 4R's and 3R's, although 8R's and others have been observed. The Sn atoms in these structures are typically bound to three oxygen atoms resulting in a trigonal pyramidal geometric configuration. There have been examples published in which the Sn atoms are 4-coordinate [28,29]; the additional bond is typically an oxygen atom at a distance of ~2.4 Å. Barrou and coworkers have synthesized a divalent Sn compound in which the Sn atom is coordinated by two oxygen atoms and two alkylamine nitrogen atoms [30]. However, prior to the work presented herein, there has not been a Sn^{II} phosphonate reported in which the Sn is additionally coordinated by a pyridyl nitrogen atom.

2. Experimental

2.1. Materials and methods

(Tetrakis)triphenylphosphine palladium, triethylamine, diethylphosphite, toluene, Sn^{II} oxalate, and 3-bromopyridine were purchased from Sigma Aldrich. Water was distilled and deionized. Toluene, triethylamine, and diethylphosphite were dried or distilled prior to use. All other starting materials were used as received. 4-Pyridylphosphonic acid [24] and 6-methyl-2-pyridylphosphonic acid [31] were synthesized as described in the literature. Thermogravimetric analyses (TGA) were performed with a TA Instruments Q500-0215 analyzer. The samples were heated from ambient temperature to 1000 °C at a rate of 10 °C per minute under air. Elemental analyses were performed by Robertson Microlit, Inc., Madison, New Jersey.

2.2. X-ray crystallography

Single crystal X-ray diffraction data for **I** were collected at 110 K on a Bruker Smart CCD-1000 diffractometer with a Mo $K\alpha$ source operated at 40 kW and 40 mV. Single crystal X-ray diffraction data for **II** were collected at 110 K on a Bruker-AXS GADDS MWPC three-circle X-ray diffractometer equipped with a rotating Cu $K\alpha$ anode operated at 40 kV and 40 mA. Single crystal X-ray diffraction data for **III** and **IV** were collected on a Bruker Smart APEX-II CCD diffractometer with a Mo $K\alpha$ source operated at 40 kV and 40 mA. Data reduction and cell refinement for all compounds were performed with SAINT [32]. SADABS [33] was used to obtain absorption corrected data. The structures were solved by direct methods using SHELXTL [34].

2.3. Syntheses

3-Pyridylphosphonic acid: $Pd(PPh_3)_4$ (2.0 mmol, 2.31 g) was placed, with a stirbar, in a 500 ml Schlenk roundbottom flask to which was then affixed a Vigreux column sealed with a septum. A needle with a balloon attached as a pressure moderator was inserted into the septum. The sealed system was then repeatedly evacuated and flushed with dry nitrogen. Toluene (30 ml) was added into the top of the condenser through the septum by syringe, and the setup was placed in an oil bath at 90 °C with stirring. Once the solid had dissolved, 3-bromopyridine (0.1 mol, 15.8 g), triethylamine (0.12 mol, 16.7 ml), and diethyl phosphite (0.12 mol, 15.5 ml) were added sequentially in the same manner as the toluene. The yellow solution was stirred and heated at 115 °C for 12 h, during which a white precipitate appeared. After cooling, 100 ml acetone was added and the mixture was filtered to remove the majority of the Et_3NHBr. The solvent was then removed under reduced pressure, and 50 ml acetone was added. After cooling to −5 °C, the mixture was filtered again to remove residual Et_3NHBr, and the acetone removed under reduced pressure. The clear brown oil was dissolved in CH_2Cl_2, dried over $MgSO_4$, and the solvent removed under reduced pressure. Column chromatography on silica gel eluted with ethyl acetate afforded 13.9 g (65% yield) diethyl 3-pyridylphosphonate. The ester was then hydrolyzed under acidic conditions according to published procedures [24]. 3-Pyridylphosphonic acid was dried *in vacuo* and used without further purification.

Diethyl 4-cyanophenylphosphonate: $Pd(PPh_3)_4$ (1.25 mmol, 1.44 g) and 4-bromobenzonitrile (50.0 mmol, 9.1 g) were placed, with a stirbar, in a 500 ml Schlenk roundbottom flask to which was then affixed a Vigreux column sealed with a septum. A needle with a balloon attached as a pressure moderator was inserted into the septum. The sealed system was then repeatedly evacuated and flushed with dry nitrogen. Toluene (50 ml) was added into the top of the condenser through the septum by syringe, and the setup was placed in an oil bath at 100 °C with stirring. A white precipitate slowly began to form. After ~20 min, an additional 10 ml toluene was added to loosen the mixture and facilitate stirring. The mixture was refluxed for 20 h, then cooled to ambient temperature before washing three times with 50 ml portions of H_2O. The clear yellow organic phase was dried over $MgSO_4$ and the solvent then removed under reduced pressure. Column chromatography on silica gel eluted with hexanes/ethyl acetate (1:1) afforded 7.2 g (79% yield) diethyl 4-cyanophenylphosphonate. The diethyl ester was used directly in the hydrothermal reaction without further purification.

Tin 3-pyridylphosphonate, $Sn(O_3PC_5NH_4)$ (**I**): In a PTFE-lined autoclave with an internal volume of 15 ml, SnC_2O_4 (0.5 mmol, 0.103 g), 3-pyridylphosphonic acid (0.5 mmol, 0.08 g), and 10 ml H_2O were heated at 180 °C for five days under autogenous pressure. After cooling, colorless crystals were collected by filtration, washed with water and ethanol, and dried in an oven at 90 °C. Yield: 0.069 g, 62% based on Sn. Anal. Calcd. for $SnO_3PC_5NH_4$: C, 21.77%; H, 1.46%; N, 5.08%. Found: C, 21.78%; H, 1.06%; N, 5.18%.

Tri-tin(μ-3)oxo-bis(4-pyridylphosphonate), $Sn_3O(O_3PC_5NH_4)_2$ (**II**): In a PTFE-lined autoclave with an internal volume of 15 ml, SnC_2O_4 (0.25 mmol, 0.052 g), 4-pyridylphosphonic acid (0.25 mmol, 0.04 g), 0.5 ml glacial acetic acid, and 10 ml H_2O were heated at 180 °C for four and a half days under autogenous pressure. After cooling, colorless crystals were collected by filtration, washed with water and ethanol, and dried in an oven at 90 °C. Yield: 0.036 g, 63% based on Sn. Anal. Calcd. for $Sn_3O_7P_2C_{10}N_2H_8$: C, 17.50%; H, 1.18%; N, 4.08%. Found: C, 17.47%; H, 1.03%; N, 3.94%.

Tin(II)-6-methyl-2-pyridylphosphonate quadrahydrate, $Sn(O_3PC_5H_3NCH_3)\cdot 0.25H_2O$ (**III**): In a PTFE-lined autoclave with an internal volume of 15 ml, SnC_2O_4 (0.40 mmol, 0.082 g), 6-methyl-2-pyridylphosphonic acid (0.40 mmol, 0.070 g), and 10 ml H_2O were heated at 145 °C for 20 h under autogenous pressure. After cooling, large pale yellow crystals and a powder of the same color were collected by filtration, washed with water and ethanol, and dried in an oven at 90 °C. Yield: 0.087 g, 74% based on Sn. Anal. Calcd. for $Sn(O_3PC_5H_3NCH_3)\cdot 0.25H_2O$: C, 24.49%; H, 2.23%; N, 4.76%. Found: C, 23.72%; H, 2.20%; N, 4.49%.

Tin(II) 4-cyanophenylphosphonate, $Sn(O_3PC_6H_4CN)$ (**IV**): In a PTFE-lined autoclave with an internal volume of 15 ml, SnC_2O_4 (0.30 mmol, 0.062 g), diethyl 4-cyanophenylphosphonate (0.30 mmol, 0.072 g), and 10 ml H_2O were heated at 145 °C for 20 h under autogenous pressure. After cooling, the white, crystalline solid was collected by filtration, washed with water and ethanol, and dried in an oven at 90 °C. Yield: 0.053 g. Reliable elemental analyses and TGA were not obtained because the sample consisted of multiple phases, as shown by powder X-ray diffraction and visual inspection of the material under a microscope. Approximately 25% of the product was identified as **IV**, based on PXRD and visual inspection. Manual separation of the phases was impractical, except for selecting a single crystal for X-ray diffraction.

3. Results

Crystallographic data for all four compounds are presented in Table 1.

3.1. Crystal Structure of *I*, $Sn(O_3PC_5NH_4)$

Compound **I** crystallizes in space group $P2_1/c$, with $\beta = 93.616(2)^\circ$. The labeling scheme and thermal ellipsoids for the 11 crystallographically independent non-hydrogen atoms are shown in Fig. 1. The Sn^{II} atoms are 3-coordinate with oxygen atoms from three separate phosphonate groups. Together, the Sn, O, and P atoms form ladders that extend along the *a*-axis. The ladders consist of fused 4-membered rings (4R's) and are decorated on top and bottom by pendant pyridyl groups (Fig. 2). The pyridyl groups are parallel to one another and canted at 35.5° from the direction of propagation of the ladder. When viewed along the *a*-axis, it can be seen that the ladders pack in a herringbone-type arrangement (Fig. 3). This arrangement allows the nitrogen atom of each pyridyl group to interact with a Sn atom from a neighboring ladder at a distance of 2.606(3) Å. The nitrogen lone pair is directed toward the Sn atom, at a position that is in between two of the Sn–O bonds and the Sn^{II} lone pair. The Sn–O bond opposite the nitrogen atom is extended to 2.218(2) Å, while the other two Sn–O bonds are only 2.095(2) and 2.097(2) Å.

3.2. Crystal Structure of *II*, $Sn_3O(O_3PC_5NH_4)_2$

Compound **II** crystallizes in space group *P*-1. The labeling scheme and thermal ellipsoids for the 24 crystallographically independent non-hydrogen atoms are shown in Fig. 4. There are two phosphonates for every three Sn atoms in the structure. Charge

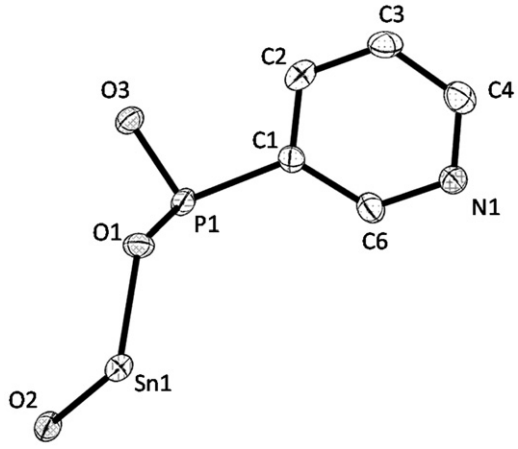

Fig. 1. Asymmetric unit of **I** with thermal ellipsoids shown at 50% probability. Hydrogen atoms have been omitted for clarity.

Table 1
Crystal data and structure refinement for complexes **I**–**IV**.

	I	II	III	IV
Chemical formula	$Sn(O_3PC_5NH_4)$	$Sn_3O(O_3PC_5NH_4)_2$	$Sn(O_3PC_6NH_6)\ 0.25H_2O$	$Sn(O_3PC_7NH_4)$
Formula mass	275.75	686.19	294.3	299.97
Crystal system	Monoclinic	Triclinic	Orthorhombic	Triclinic
Space group	$P2_1/c$	$P\bar{1}$	$Pna2_1$	$P\bar{1}$
a (Å)	4.9595(8)	7.2406(14)	18.955(3)	5.0019(3)
b (Å)	10.7673(18)	9.9524(19)	9.7543(14)	8.4396(5)
c (Å)	13.996(2)	12.604(3)	17.833(3)	10.3099(6)
α (deg.)	90.00	104.510(11)	90.00	90.352(3)
β (deg.)	93.616(2)	90.326(11)	90.00	94.894(3)
γ (deg.)	90.00	110.897(11)	90.00	92.236(4)
Z	4	2	4	2
V (Å^3)	745.9(2)	816.9(3)	3297.2(9)	433.29(4)
Density (g/cm^3)	2.456	2.790	2.367	2.298
Measured reflections	8139	6200	65018	6570
Unique reflections	1635	2167	10881	1686
Parameters	100	218	447	131
$R_1 > 2\sigma(I)$, wR_2	0.0224, 0.0381	0.0391, 0.1070	0.0300, 0.0625	0.0324, 0.0673
S (GooF) all data	1.024	1.001	1.07	1.078
Max/min res. dens. (e/Å^3)	0.696, −0.550	1.105, −1.521	1.126, −1.071	0.837, −0.863

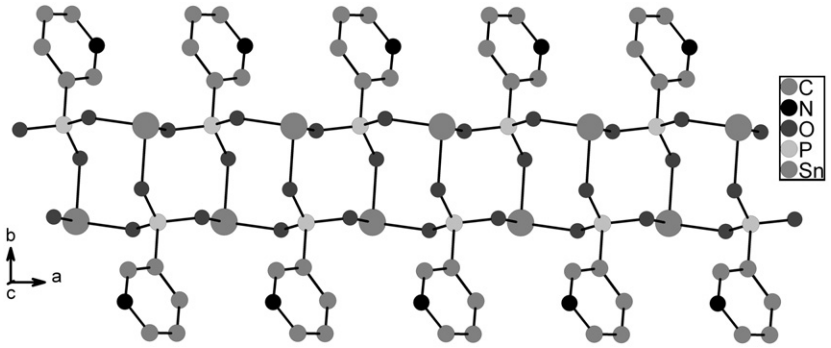

Fig. 2. Fused 8-membered rings (4R's) form ladders in **I**.

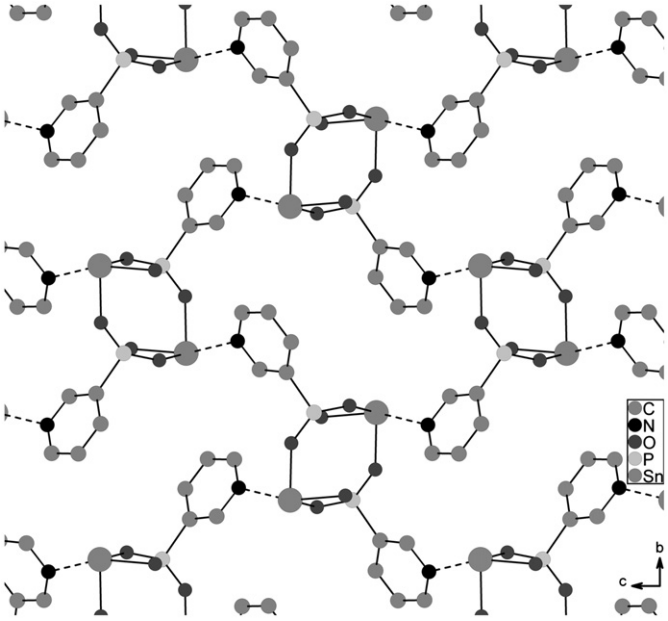

Fig. 3. The chains of **I** pack in a herringbone-type arrangement to allow for the Sn–N interaction at ~2.6 Å.

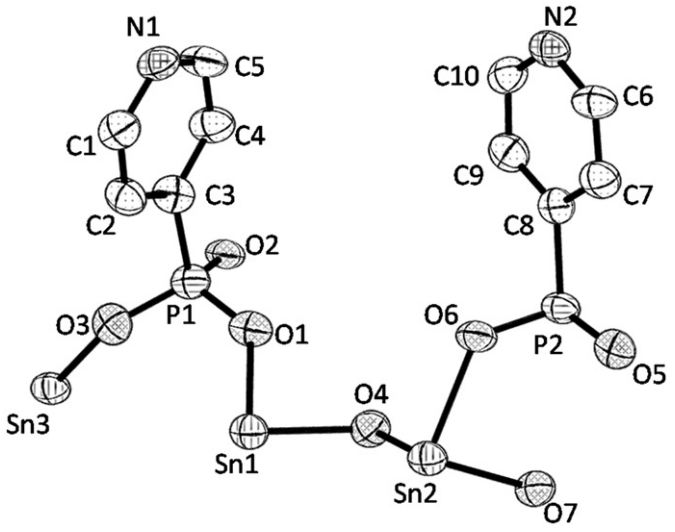

Fig. 4. Asymmetric unit of **II** with thermal ellipsoids shown at 50% probability. Hydrogen atoms have been omitted for clarity.

balance is achieved by the incorporation of an O^{2-} atom, which is not observed for any of the other compounds presented in this study. The Sn atoms are all coordinated by three oxygen atoms: the O^{2-} and two oxygen atoms from two different phosphonate groups. The O^{2-} is bonded to Sn1, Sn2, and Sn3 at distances of 2.080(6), 2.083(6), and 2.090(6) Å, respectively. Two of the Sn–O–Sn bond angles are similar (Sn2–O4–Sn3 = 121.87°, Sn1–O4–Sn3 = 121.09°), but one is relatively contracted (Sn1–O4–Sn2 = 112.52°). This creates a situation which requires the O^{2-} atom to be pyramidally distorted from trigonal planar geometry, and slightly pushed out of the plane formed by the three Sn atoms. The Sn, O, and P atoms form ladders that extend along the *c*-axis, which consist of fused 4R's and 3R's, with O4 and Sn3 being shared by two 3R's. The pyridyl groups extend above and below the ladders, at a slight angle to the next pyridyl group on the ladder (Fig. 5). Nearest-neighbor pyridyl groups on the ladders are nearly perpendicular to one another, but next-nearest neighbor pyridyl groups are parallel. Each pyridyl group is oriented so that the N lone pair is directed toward a Sn atom from an adjacent ladder. The Sn–N distances are 2.690(6) Å for Sn1–N1 and 2.618(6) Å for Sn2–N2. As in compound **I**, the pyridyl nitrogen lone pairs are directed at the Sn atoms from a position in between two Sn–O bonds and the Sn^{II} lone pair. The Sn–O bonds opposite the Sn–N bonds are lengthened compared to the other Sn–O bonds: 2.225(6) Å for Sn1–O2 and 2.250(6) Å for Sn2–O6. The other Sn–O bond lengths are 2.080(6), 2.118(6), 2.083(6), and 2.118(6) Å for Sn1–O4, Sn1–O1, Sn2–O4, and Sn2–O7, respectively. The pyridyl groups from a single ladder interact with Sn atoms from four adjacent ladders. These interactions are most easily seen when the structure is viewed from along the *c*-axis (Fig. 6). The pyridyl groups from different ladders are oriented parallel to and facing one another at a distance of ~3.5 Å, an indication that there is a reasonably strong π–π interaction (Fig. 7).

3.3. Crystal Structure of ***III***, $Sn(O_3PC_5H_3NCH_3)\ 0.25H_2O$

Compound **III** crystallizes in orthorhombic space group $Pna2_1$. The labeling scheme and thermal ellipsoids for the 49 crystallographically independent non-hydrogen atoms are shown in Fig. 8. Each of the four distinct Sn atoms in the structure is four-coordinate: two are coordinated only by phosphonate oxygen atoms and two are coordinated by two phosphonate oxygen atoms and two pyridyl nitrogen atoms. The Sn–O and Sn–N bond distances are reported in Table 2. Each Sn atom has two short (~2.1 Å) Sn–O bonds and two longer bonds. For Sn1 and Sn3, the longer bonds are with nitrogen atoms, and for Sn2 and Sn4, the longer bonds are with two additional oxygen atoms. The Sn, O, and P atoms form 2-D sheets made of fused 4R's and 8R's (Fig. 9). The pyridyl nitrogen atoms interact only with Sn atoms in the same layer, so there are no interlayer bonds holding the sheets together. The layers pack in an interlocking fashion so the methylpyridyl

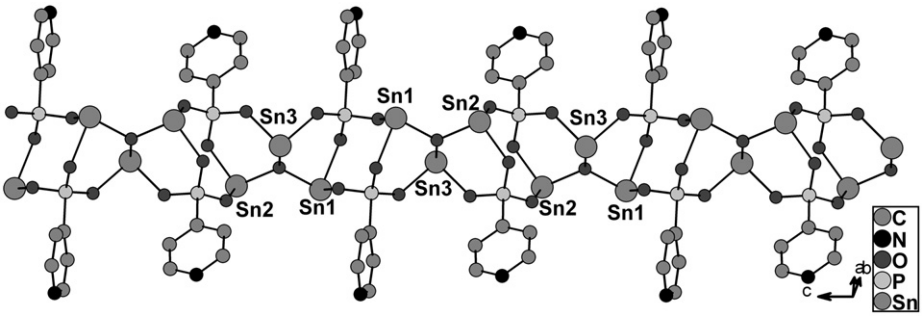

Fig. 5. View of **II** showing ladders formed by fused rings. The 3R's share the μ-3 oxygen and a Sn atom. Hydrogen atoms have been omitted for clarity.

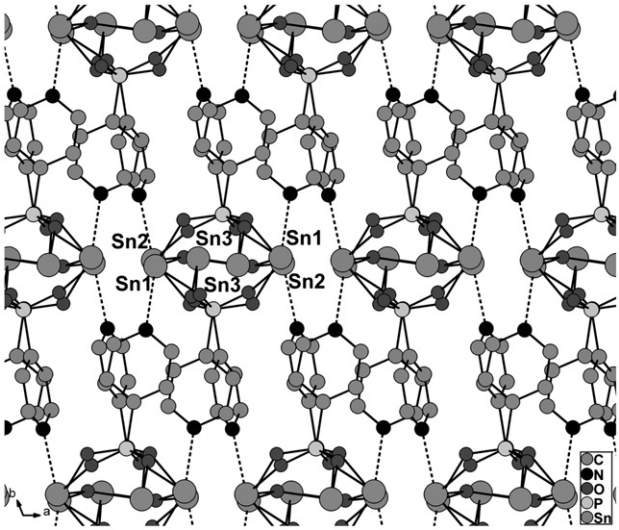

Fig. 6. View along the *c*-axis of the ladders in **II**, showing the Sn–N interactions. Hydrogen atoms have been omitted for clarity.

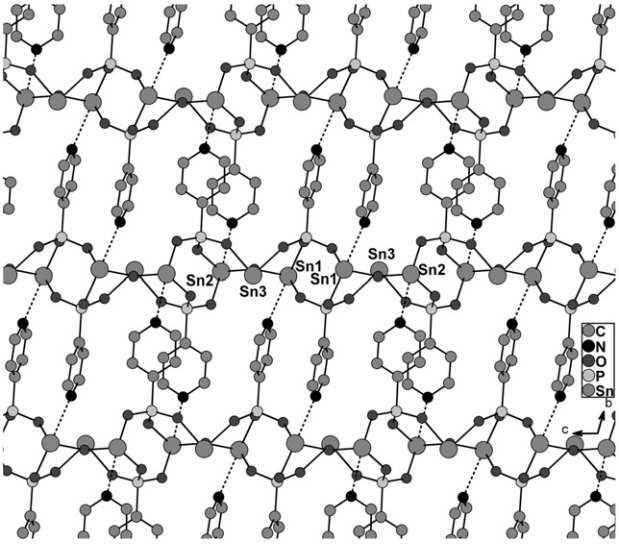

Fig. 7. View showing the interaction between the chains in **II**. Sn–N interactions are depicted as dotted lines. Note the π–π stacking arrangement of the pyridyl rings. Hydrogen atoms have been omitted for clarity.

groups from one layer fit in between those of an adjacent layer (Fig. 10). The single solvent water molecule is located between the layers. No other solvent water molecules could be located.

3.4. Crystal Structure of **IV**, $Sn(O_3PC_6H_4CN)$

Compound **IV** crystallizes in space group *P*-1. The labeling scheme and thermal ellipsoids for the 13 crystallographically independent non-hydrogen atoms are shown in Fig. 11. The phenyl ring is rotationally disordered around the C1–C4 axis, with each component contributing equally to the total occupancy. Each Sn atom is 3-coordinate with oxygen atoms from three different phosphonate groups, and the Sn, O, and P atoms form ladders that extend along the *a*-axis, as in compound **I**. The ladders are essentially identical to those of **I**, with the major difference being the pendant organic moieties that decorate the top and bottom of the ladders (Fig. 12). In **III**, all three Sn–O bonds are similar; 2.103(3), 2.118(3), and 2.132(4) Å for Sn1–O2, Sn1–O3, and Sn1–O1, respectively. The nitrile lone pairs do not point directly at the Sn atoms, and the shortest Sn–N distance is >3.2 Å. The ladders pack in a side-by-side manner that does not facilitate a Sn–N interaction (Fig. 13).

3.5. TGA analyses

TGA analyses were performed on compounds **I**–**III**. The samples were ground with a mortar and pestle prior to heating.

Compound **I** shows no evidence of decomposition until ~325 °C, at which point a weight increase is seen, corresponding to the oxidation of Sn^{II} to Sn^{IV} and the concurrent uptake of oxygen from the air. The organics combust between 450 and 650 °C, before the final weight loss event occurs over a large range centered at ~800 °C. The observed weight loss is 19.75%, which is in agreement with the calculated weight loss (19.61%) for the complete conversion to an equimolar mixture of SnO_2 (ICDD card number 41-1445) and $Sn(P_2O_7)$ (ICDD card number 29-1352).

Compound **II** shows its first weight loss at ~500 °C, due to the combustion of the pyridyl rings. The oxidation of Sn^{II} occurs during this step, as evidenced by a large negative spike in the derivative weight change at ~525 °C. The second major weight loss at ~750 °C corresponds to the phosphonate groups splitting out water and forming $P_2O_7^{4-}$. The calculated weight loss for the complete conversion to $2SnO_2$ and $Sn(P_2O_7)$ is 13.43%, which is close to the observed loss of 14.19%.

Compound **III** gradually loses 1/4 of a water molecule per formula unit as it is heated from 25 to 400 °C, corresponding with a loss of 1.53%. The organic groups combust in two steps between 400 and 600 °C, and the material undergoes a final decomposition step centered at ~800 °C as the pyrophosphate forms and water is split out. The observed weight loss of 23.64% is reasonably consistent with the calculated loss of 24.70% for the complete conversion to an equimolar mixture of SnO_2 and $Sn(P_2O_7)$.

It is worthy of note that the oxidation of Sn^{II} and the accompanying weight increase (due to reaction with oxygen from

the air) in **III** occurs slightly before the decomposition of the organic groups. This is also observed for compound **I**, but in that case, the increase is broad and drawn out over a range between 300 and 500 °C. The oxidation of Sn^{II} in compound **III** is rapid, occurring between 400 and 450 °C. We suspected that the broadness of the increase for **I** relative to that of **III** was perhaps due to a larger average particle size caused by variations in sample preparation. However, the TGAs were repeated after carefully and fully grinding the samples and the same results were obtained.

4. Discussion

The initial aim of this work was to create a layered compound possessing Lewis base functionality in the form of pyridyl groups, which would be available to coordinate and sequester metal ions. In Sn^{II} phenylphosphonate, phenyl groups decorate both sides of infinite Sn–O–P layers [35]. It seemed plausible that by substituting a pyridylphosphonic acid for phenylphosphonic acid, it would create an isostructural compound having pyridyl nitrogen lone pairs directed into the interlayer space. This material could then coordinate nitrophilic metals, which might lead to useful catalytic or ion-exchange properties. However, the structure of Sn^{II} 3-pyridylphosphonate is different from that of Sn^{II} phenylphosphonate. Instead of 2-D sheets, the structure of Sn^{II} 3-pyridylphosphonate consists of fused-ring ladders decorated by pendant pyridyl groups. The Sn–N distance is relatively short (~2.6 Å), and the pyridyl N atoms are pointing almost directly at the Sn atoms. Changing the position of the N atom from 3- to 4- within the pyridyl ring yields a different structure.

The ladders in **I** are arranged so that the pyridyl nitrogen lone pairs can donate to the Sn atoms of adjacent ladders. The Sn–O bond opposite to the pyridyl N-donor is lengthened by more than 0.1 Å, reflecting the Sn–O antibonding character of the Sn–N bonding orbital. This is also observed in compounds **II** and **III**. In each of these instances, Sn^{II} is acting as a Lewis acid, which is an unusual role for a metal that, in the divalent state, usually acts as a Lewis base by donating its 5*s* lone pair. It should be pointed out that although the Sn^{II} atoms possess a lone pair, they are also coordinatively unsaturated, thus their tendency to interact with the donor nitrogen atoms. We tested the strength of this tendency by incorporating a nitrile group into the phosphonic acid, which yielded **IV**. In this compound, there is no Sn–N interaction, perhaps because nitrile is a much weaker base than pyridyl. The same ladder motif forms in both **I** and **IV**, but in **I**, the ladders are packed in a herringbone-type arrangement to allow for the Sn–N interaction. In compound **IV**, the absence of this interaction allows the ladders to pack in a simple side-by-side fashion. We have not determined why **IV** adopts a ladder structure instead of a

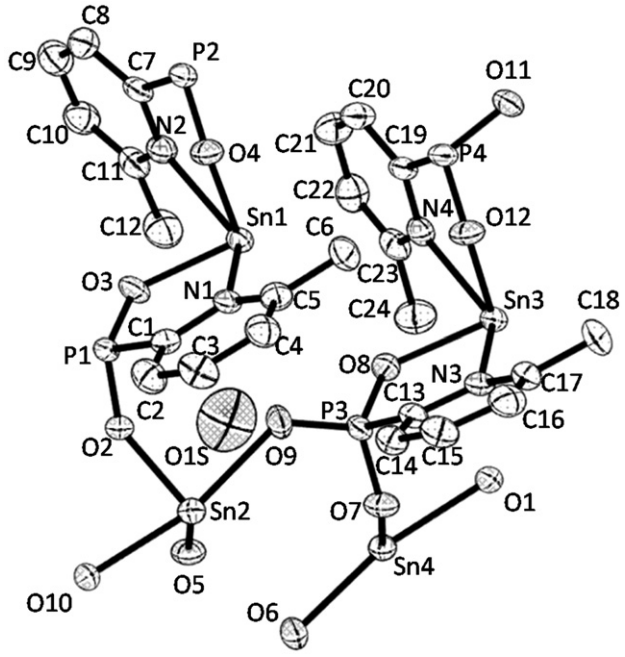

Fig. 8. Asymmetric unit of **III** with thermal ellipsoids shown at 50% probability. Hydrogen atoms have been omitted for clarity.

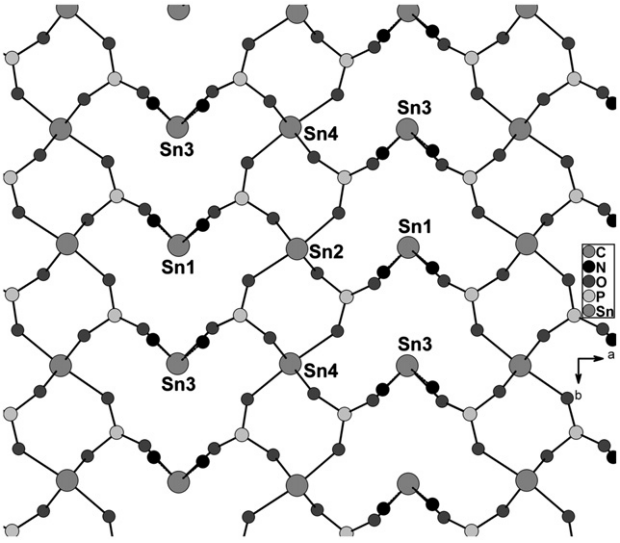

Fig. 9. View from above one layer of **III** showing the 4R's and 8R's. The carbon and hydrogen atoms have been removed for clarity. All Sn^{II} atoms are four-coordinate.

Table 2
Selected bond distances for compounds **I–IV.**

Compound	Atom pair	Distance (Å)	Atom pair	Distance (Å)	Atom pair	Distance (Å)
I	Sn1–O1	2.099(2)	Sn1–O2	2.095(2)	Sn1–O3	2.218(2)
II	Sn1–O1	2.118(6)	Sn1–O2	2.225(6)	Sn1–O4	2.080(6)
	Sn2–O4	2.083(6)	Sn2–O6	2.250(6)	Sn2–O7	2.118(6)
	Sn3–O3	2.142(6)	Sn3–O4	2.090(6)	Sn3–O5	2.110(6)
III	Sn1–O3	2.124(2)	Sn1–O4	2.134(2)	Sn1–N1	2.454(3)
	Sn1–N2	2.620(3)	Sn2–O2	2.101(2)	Sn2–O5	2.105(2)
	Sn2–O10	2.279(2)	Sn2–O9	2.423(2)	Sn3–O12	2.138(2)
	Sn3–O8	2.141(2)	Sn3–N4	2.469(3)	Sn3–N3	2.555(3)
	Sn4–O7	2.096(2)	Sn4–O11	2.108(2)	Sn4–O1	2.317(2)
	Sn4–O6	2.397(2)				
IV	Sn1–O1	2.132(4)	Sn1–O2	2.103(3)	Sn1–O3	2.118(3)

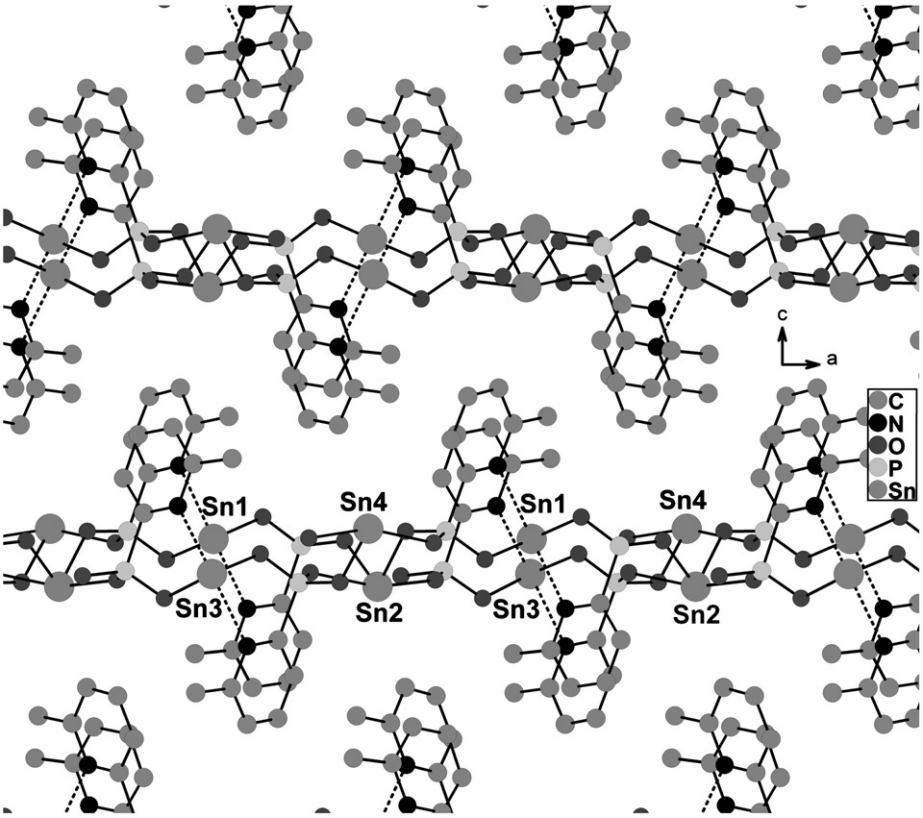

Fig. 10. View of compound **III** showing the interlocking layers. The solvent water has been removed for clarity.

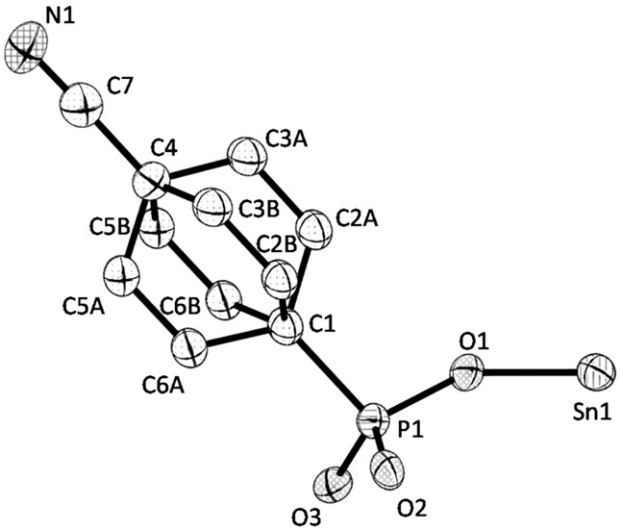

Fig. 11. Asymmetric unit of **IV** with thermal ellipsoids at 50% probability. The phenyl ring is disordered, with each part at 50% occupancy. Hydrogen atoms have been omitted for clarity.

layered structure, even though there is not a Sn–N interaction. In the original work [35], Sn phenylphosphonate was synthesized at high temperature in the presence of HF and DMSO. We obtained no solid materials when these conditions were used in an attempt to synthesize a layered polymorph of **IV**, probably because the nitrile group is prone to decomposition at elevated temperatures and at low pH. We attempted to synthesize a ladder polymorph of Sn phenylphosphonate by subjecting the mixture to milder conditions and foregoing the use of HF, but even under these much milder conditions, the layered structure was obtained. The fact that the same ladder units appear in both **I** and **IV**, but are packed differently shows that the Sn–N interaction is strong enough to alter the final structure of Sn phosphonates, which are typically robust, stable materials.

This work is the first example of a Sn^{II} phosphonate in which the Sn atoms are four-coordinate with three O atoms and one pyridyl N atom (**I** and **II**). Another novel coordination environment occurs in **III**, in which the Sn^{II} is four coordinate with two O atoms and two N atoms from pyridyl rings.

We attempted to interrupt the Sn–N interaction in **I** by including acetic acid in the reaction mixture, thinking that the pyridine would then be protonated and unable to coordinate to the Sn atoms. The compound obtained was identical to that obtained without acetic acid. Although no acetate was included in the structure, a greater fraction of the material obtained was crystalline, and the crystals were larger than those obtained without acetic acid. It may be that the acetic acid helps to dissolve the SnC_2O_4, which is only sparingly soluble in pure water. Hydrothermal reactions carried out with $SnCl_2 \cdot 2H_2O$ (as a source of HCl to protonate the pyridine) instead of SnC_2O_4 were not successful, resulting only in liquids that failed to yield crystals upon slow evaporation. We are continuing efforts to interrupt the Sn–N interaction and more completely understand the structure-directing influences at work. If the Sn–N interaction can be selectively interrupted, then it may be possible to use the ladders as secondary building units in more complex materials.

We could not find any published examples of Sn phosphonates that contain the $Sn_3(\mu\text{-}3)$-oxo unit that is present in compound **III**. However, Davies and coworkers [36] reported the structure of tritin(II) dihydroxide oxide sulphate, which contains the $[Sn_3O(OH)_2]^{2+}$ cation. In that structure, the oxygen atom is central and coordinated only by three Sn atoms at distances of

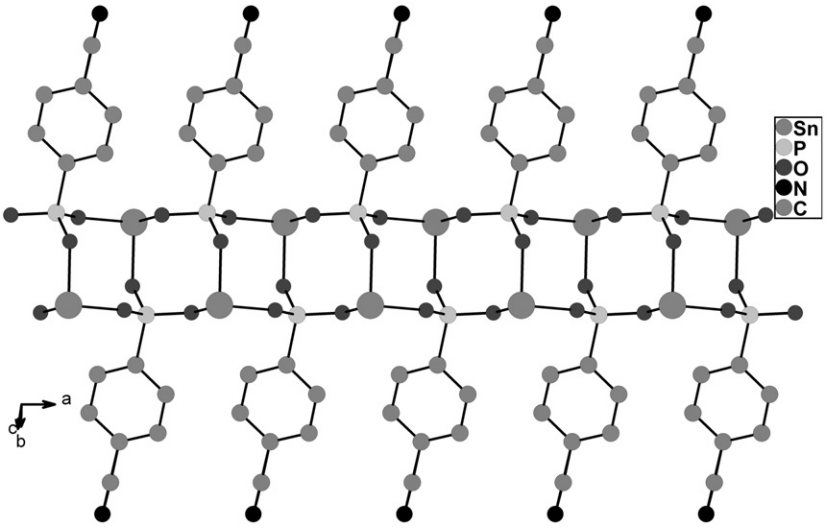

Fig. 12. View showing ladders in **IV**, which are essentially the same as those in **I**.

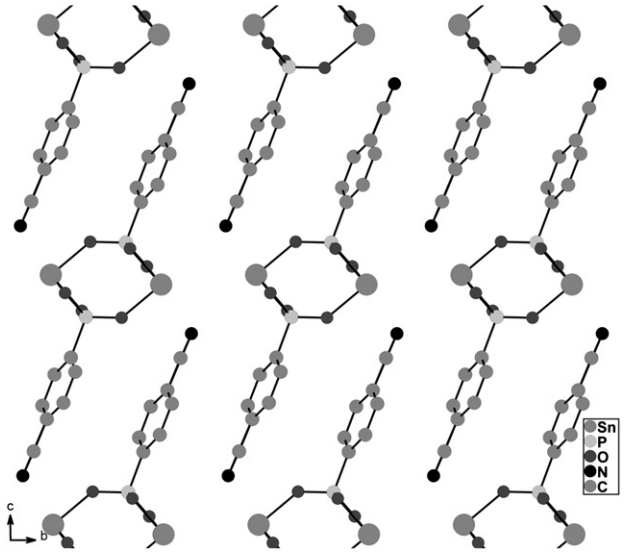

Fig. 13. The packing arrangement of the chains in **IV**. Note the lack of a direct Sn–N interaction. For the sake of clarity, only one position of the rotationally disordered phenyl ring is shown.

2.062(7), 2.063(7), and 2.094(8) Å. These distances are similar to the Sn–O distances reported herein for compound **III**: 2.080(6), 2.083(6), and 2.090(6) Å. In addition, Natarajan and Cheetham [37] encountered the $Sn_3(\mu\text{-}3)$-oxo unit in the structure of $[NH_4]^+[(Sn_3O_2)(PO_4)_3]^-$. They report similar values for the Sn–O distances. Like **III**, both of these compounds were obtained from reactions in water, so it is likely that the solvent is the source of the O^{2-} incorporated into the structure.

5. Conclusion

We have shown that the relatively weak interaction between a pyridyl N and Sn^{II} can have profound consequences on the structures of tin(II) phosphonates. This influence demonstrates the significant effects that a minor change in the ligand can have on the formation of metal organic frameworks. Future work will focus on this subtle interaction in other materials, as well as exploring ways to selectively interrupt it to modify the structure and obtain new compounds. Chemists working with hybrid materials typically focus on varying the geometry of the ligands and the arrangement of the functional groups which coordinate metals to influence the architecture of the products. We must recognize that the functional groups we incorporate into hybrid materials are not simply innocent bystanders, and may actually allow us greater control over the final structures of these promising materials.

Acknowledgments and Funding

The authors thankfully acknowledge the National Science Foundation (Grant DMR-0652166) and the Robert A. Welch Foundation (Grant A0673) for financial support. The work in Wroclaw was supported by the Ministry of Science and Higher Education (Poland) and Wroclaw University of Technology.

Appendix A. Supporting Information

Supporting information available: Crystallographic files in CIF format for **I–IV** and TGA graphs for **I–III** are available free of charge via the internet at doi:10.1016/j.jssc.2010.03.016.

References

[1] K. Barthelet, J. Marrot, D. Riou, G. Ferey, Angewandte Chemie, International Edition 41 (2) (2002) 281–284.
[2] S.R. Caskey, A.G. Wong-Foy, A.J. Matzger, Inorganic Chemistry 47 (17) (2008) 7751–7756.
[3] H.K. Chae, D.Y. Siberio-Perez, J. Kim, Y.B. Go, M. Eddaoudi, A.J. Matzger, M. O'Keeffe, O.M. Yaghi, Nature 427 (6974) (2004) 523–527.
[4] M. Eddaoudi, J. Kim, N. Rosi, D. Vodak, J. Wachter, M. O'Keeffe, M. Yaghi Omar, Science 295 (5554) (2002) 469–472.
[5] G. Ferey, Science 291 (5506) (2001) 994–995.
[6] G. Ferey, C. Mellot-Draznieks, C. Serre, F. Millange, Accounts of Chemical Research 38 (4) (2005) 217–225.
[7] G. Ferey, C. Mellot-Draznieks, C. Serre, F. Millange, J. Dutour, S. Surble, I. Margiolaki, Science 309 (5743) (2005) 2040–2042.
[8] F. Millange, C. Serre, G. Ferey, Chemical Communications (8) (2002) 822–823.
[9] J.L.C. Rowsell, A.R. Millward, K.S. Park, O.M. Yaghi, Journal of the American Chemical Society 126 (18) (2004) 5666–5667.
[10] O.M. Yaghi, M. O'Keeffe, N.W. Ockwig, H.K. Chae, M. Eddaoudi, J. Kim, Nature 423 (6941) (2003) 705–714.
[11] A. Cabeza, M.d.M. Gomez-Alcantara, P. Olivera-Pastor, I. Sobrados, J. Sanz, B. Xiao, R.E. Morris, A. Clearfield, M.A.G. Aranda, Microporous and Mesoporous Materials 114 (1–3) (2008) 322–336.
[12] A. Clearfield, Dalton Transactions (44) (2008) 6089–6102.

[13] Z. Wang, J.M. Heising, A. Clearfield, Journal of the American Chemical Society 125 (34) (2003) 10375–10383.
[14] H. Furukawa, M.A. Miller, O.M. Yaghi, Journal of Materials Chemistry 17 (30) (2007) 3197–3204.
[15] Y. Li, T. Yang Ralph, Langmuir 23 (26) (2007) 12937–12944.
[16] U. Mueller, M. Schubert, F. Teich, H. Puetter, K. Schierle-Arndt, J. Pastre, Journal of Materials Chemistry 16 (7) (2006) 626–636.
[17] A. Clearfield, Z. Wang, Journal of the Chemical Society, Dalton Transactions (15) (2002) 2937–2947.
[18] M.J. Ingleson, J.P. Barrio, J. Bacsa, C. Dickinson, H. Park, M.J. Rosseinsky, Chemical Communications (11) (2008) 1287–1289.
[19] J. Wu, H. Hou, H. Han, Y. Fan, Inorganic Chemistry 46 (19) (2007) 7960–7970.
[20] P. Ayyappan, O.R. Evans, B.M. Foxman, K.A. Wheeler, T.H. Warren, W. Lin, Inorganic Chemistry 40 (23) (2001) 5954–5961.
[21] J.A. Fry, C.R. Samanamu, J.-L. Montchamp, A.F. Richards, European Journal of Inorganic Chemistry (3) (2008) 463–470.
[22] B. Chen, C. Liang, J. Yang, D.S. Contreras, Y.L. Clancy, E.B. Lobkovsky, O.M. Yaghi, S. Dai, Angewandte Chemie, International Edition 45 (9) (2006) 1390–1393.
[23] M. Shanmugam, M. Shanmugam, G. Chastanet, R. Sessoli, T. Mallah, W. Wernsdorfer, R.E.P. Winpenny, Journal of Materials Chemistry 16 (26) (2006) 2576–2578.
[24] S. Konar, J. Zon, A.V. Prosvirin, K.R. Dunbar, A. Clearfield, Inorganic Chemistry 46 (13) (2007) 5229–5236.
[25] P.J. Zapf, D.J. Rose, R.C. Haushalter, J. Zubieta, Journal of Solid State Chemistry 125 (2) (1996) 182–185.
[26] A. Subbiah, N. Bhuvanesh, A. Clearfield, Journal of Solid State Chemistry 178 (4) (2005) 1321–1325.
[27] B.A. Adair, S. Neeraj, A.K. Cheetham, Chemistry of Materials 1 (7) (2003) 1518–1529.
[28] B. Adair, S. Natarajan, A.K. Cheetham, Journal of Materials Chemistry 8 (6) (1998) 1477–1479.
[29] N. Stock, G.D. Stucky, A.K. Cheetham, Chemical Communications (22) (2000) 2277–2278.
[30] N.N. Zemlyansky, I.V. Borisova, M.G. Kuznetsova, V.N. Khrustalev, Y.A. Ustynyuk, M.S. Nechaev, V.V. Lunin, J. Barrau, G. Rima, Organometallics 22 (8) (2003) 1675–1681.
[31] D. Redmore, Journal of Organic Chemistry 35 (12) (1970) 4114–4117.
[32] H. Oshio, N. Hoshino, T. Ito, M. Nakano, F. Renz, P. Gutlich, Angewandte Chemie, International Edition 42 (2) (2003) 223–225.
[33] G.M. Sheldrick, SADABS, Program for Absorption Correction of Area Detector Frames, Bruker AXS, Inc., Madison, WI.
[34] G.M. Sheldrick, Acta Crystallographica, Section A Foundations of Crystallography A 64 (1) (2008) 112–122.
[35] D.E. Lansky, P.Y. Zavalij, S.R.J. Oliver, Acta Crystallographica, Section C: Crystal Structure Communications C 57 (9) (2001) 1051–1052.
[36] C.G. Davies, J.D. Donaldson, D.R. Laughlin, R.A. Howie, R. Beddoes, Journal of the Chemical Society Dalton Transactions Inorganic Chemistry 1975 (21) (1972–1999) 2241–2244.
[37] S. Natarajan, A.K. Cheetham, Journal of Solid State Chemistry 134 (1) (1997) 207–210.